J Solid State Electrochem (2004) 8: 968–975
DOI 10.1007/s10008-004-0526-9

ORIGINAL PAPER

J. Mathiyarasu · A. M. Remona · A. Mani
K. L. N. Phani · V. Yegnaraman

Exploration of electrodeposited platinum alloy catalysts for methanol electro-oxidation in 0.5 M H_2SO_4: Pt-Ni system

Received: 22 November 2003 / Accepted: 11 March 2004 / Published online: 20 April 2004

Abstract In this work, we examine the electrocatalytic activity of electrodeposited Platinum (Pt)-Nickel (Ni) alloy layers on an inert substrate electrode for methanol oxidation reaction. Analyses using energy-dispersive fluorescent X-ray analysis and powder X-ray diffractometry confirm alloying of Pt with Ni in a range of compositions. Steady-state polarisation measurements in 0.5 M methanol + 0.5 M H_2SO_4 solutions clearly show that the onset of electro-oxidation shifts to less anodic potential values (approximately 160 mV), while also exhibiting current enhancements up to ~15 times the currents obtained for the pure Pt electrodeposit. A linear relationship between the cyclic voltammetric peak (oxidation) current and [MeOH] is observed at a scan rate of 50 mVs^{-1}, thus indicating reduced influence of adsorbed CO (CO_{ads}) surface poison. A critical composition, Pt (92%)/Ni (8%) [denoted Pt-Ni(3) alloy] is found to exhibit maximum electrocatalytic activity, beyond which the activity drops, whereas pure Ni does not catalyse the reaction. While the promotion of electro-oxidation is understood to be *largely* due to the alloy catalyst, surface redox species of Ni oxide formed during the electro-oxidation process may also contribute to the oxygenation of CO_{ads}, thereby enhancing the oxidation current. Plausible mechanisms of methanol oxidation on Pt/ transition metal alloy electrocatalysts are discussed in terms of electron transfer (in the alloy) and the role of Ni oxide species.

J. Mathiyarasu (✉) · A. M. Remona · K. L. N. Phani
V. Yegnaraman
Electrodics and Electrocatalysis Division,
Central Electrochemical Research Institute,
630 006 Karaikudi, India
E-mail: al_mathi@yahoo.com
Fax: +91 4565 227779

A. Mani
X-ray Diffraction Laboratory,
Central Electrochemical Research Institute,
630 006 Karaikudi, India

Keywords Platinum-nickel · Electrodeposition · Cyclic voltammetry · Methanol oxidation

Introduction

Exploration of alloy catalyst combinations for efficient electro-oxidation of small organic molecules, especially methanol, is currently a worldwide activity in the context of direct methanol fuel cells [1, 2, 3, 4, 5, 6, 7, 8, 9]. The role of the secondary metal catalyst (e.g. ruthenium) is to promote oxygenation of the surface poison, adsorbed CO (CO_{ads}), on platinum (Pt) and thus enhance the overall catalytic activity [10, 11, 12, 13, 14]. Recent theoretical calculations have pointed to the possibility of arriving at catalyst combinations alternative to ruthenium along with Pt electrocatalysts [15].

There is considerable current interest in screening of Pt alloys for the electro-oxidation of methanol and related small organic molecules, Pt-Ru being the benchmark alloy electrocatalyst. This is mainly due to the fact that the reasons for the best performance of Ru (along with Pt) have been uncovered only recently [16, 17]. It is now known that Ru does not exist in its zero oxidation state when the alloy is in contact with an electrolyte solution and that it is instead in an oxyhydroxy form [16, 17], while also providing mixed (electronic and ionic) conductivity [16]. These studies open up new avenues for discovering alloying elements equivalent to or better than Ru. Hence, the interest has shifted to alloys of Pt with other transition metals. The initial attempts in finding alternatives to Ru included a combinatorial approach to screen such alloys and hence, new roles have been assigned to elements like Os and Ir [18]. However, studies on alloying elements other than Ru are scarce. Much lies in the selection of such alloys in identifying transition metals that might provide the same beneficial effect as provided by Ru. The key to such catalytic enhancement is (a) the stability of the transition metal on the surface at methanol oxidation reaction (MOR)

conditions, and (b) achieving the optimum surface composition. Prompted by model calculations [19] and bonding energy data, Park et al [20] recently have reported studies on Pt-Ni alloy nanoparticle films on a gold electrode surface for methanol oxidation. These particles were synthesised by chemical reduction of Pt- and Ni-salts in an aqueous medium. The results of these studies were compared with the behaviour of electrocatalysts like Ni-Ti [21], Pt-Ni [22], pure Ni [23, 24] and pure Pt [25] in acid and alkaline media, but not with the bulk alloy electrocatalysts (as has been done in the case of oxygen reduction) [26]. However, the issue of explaining the main characteristics of Pt-Ni, (i.e. for systems other than Ru) by the bifunctional mechanism is raised by Park et al [20] considering the differences in the bonding energies of Ru-O and Ni-O vis-à-vis Pt-C. Thus, a study involving bulk alloy electrocatalysts becomes necessary at this juncture and hence forms an important part of our current efforts. For practical reasons, it is preferable to choose a method that affords benefits such as ease of immobilisation on inert surfaces, good adherence and feasibility to control the size and loading particles. Electrodeposition is an established technique for obtaining alloys of different compositions on the electrode surface, and fits into this category of catalyst immobilisation strategies.

The present work is aimed at studying the role of Ni in the electrodeposited films of Pt-Ni on the electrooxidation of methanol.

Materials and methods

Electrodeposition of alloy catalyst layer The catalytic films were electrochemically deposited from a deposition mixture comprising 0.01 M $H_2PtCl_6.xH_2O$ and varying concentrations of $NiCl_2.6H_2O$ (0.01–0.50 M) at 25 °C. Before deposition, the Au electrode was polished with alumina paste and washed ultrasonically in Millipore water (18 MΩ cm). It was then subjected to electrodeposition at a fixed potential of −1.2 V versus a saturated calomel electrode (SCE) for a duration of 10 min. After deposition, the working electrode was washed thoroughly with Millipore water and dried before further investigation.

The electrochemical cell used in this work was a conventional three-compartment cell. A large surface area Pt sheet and mercury-mercurous sulphate electrode (MSE) ($Hg/HgSO_4$/0.5 M H_2SO_4) were used as the counter and reference electrodes respectively. A gold disc electrode of 4 mm diameter (Bioanalytical Systems), which is electrodeposited with Pt/Pt-Ni films served as the working electrode. All chemicals were analytical grade and used as obtained without further purification.

Cyclic voltammetry was performed using a potentiostat (PINE, Model AFRDE 5 Bipotentiostat) coupled to an X-Y/t recorder (Rikadenki RW 201T). Polarisation and chronoamperometric experiments were performed with a Solartron Electrochemical interface Model SI 1287.

Characterisation of catalyst layer The resulting electrodeposits were analysed using X-ray diffractometry (JEOL 8030 diffractometer with CuK_α(Ni-filtered) radiation ($\lambda = 1.5418$ A°) at a rating of 40 kV and 20 mA). The approximate film composition (±2 atomic%) was analysed with an energy-dispersive fluorescent X-ray analysis (XRF-EDX) (Horiba X-ray analytical microscope XGT-2700). A scanning electron microscope (Hitachi-S3000H) was used to study the morphology of the electrodeposited Pt/Pt-Ni films.

Results and discussion

Electrodeposition of Pt and Pt-Ni and characterisation

Pt-Ni catalyst layers were electrodeposited on the Au electrode surface from a plating bath containing $H_2PtCl_6.xH_2O$ and varying concentrations of $NiCl_2.6H_2O$ [27] at −1.2 V versus the SCE at 25 °C. A polycrystalline Au surface is chosen as the working electrode since (a) it is electrocatalytically inactive towards methanol oxidation and adsorption, and (b) it presents a reproducible *signature* of its oxidation/reduction in voltammetry. Before plating of Pt or Pt-Ni, the cleanliness of the polycrystalline gold electrode was ensured by checking its standard voltammetric response and its associated charge values during oxidation and reduction in the first cycle. Upon the deposition of Pt layers, the standard voltammetric response of Au disappeared and the electrode assumed the response typical of polycrystalline Pt, consisting of the well-known reversible H_{upd} region (−0.65 to −0.4 V versus MSE) and Pt oxidation/reduction (0.0–0.1 V vs MSE). Methanol was found to undergo oxidation at this electrode with voltammetric features similar to those reported in the literature [28].

The electrodeposited layers were subjected to characterisation by XRF-EDX to find out the approximate Pt:Ni ratio. Different ratios of Ni could be deposited along with Pt by keeping the concentration of H_2PtCl_6 constant and varying that of $NiCl_2$ in the plating bath. The compositions of these alloys are listed in Table 1.

Figure 1 shows the X-ray diffraction patterns of the electrodeposited Pt and Pt-Ni matrix that clearly show the characteristic peaks of Pt *fcc* structure. The intensity of the Pt characteristic peaks such as (111), (200), (220), and (311) decreases as the Ni content increases in the film. As can be noted from the diffractograms, no characteristic lines of Ni *fcc* structure are observed. The absence of lines corresponding to metallic Ni *fcc* structure (along with Pt lattice) may be due to the metallic grains that are intermixed with amorphous Ni oxides such as NiO, $Ni(OH)_2$and Ni(O)OH [16]. For the Pt component of the deposited film, the 2θ value of (111), (200), (220), (311) shows a shift in angle when compared to pure Pt (Table 2). The higher shift in 2θ value of the

Table 1 XRF-EDX analysis of electrodeposited PtNi catalytic surface films

Description	Platinum (%)	Nickel (%)
Pt	100	—
Pt-Ni(1)	96	4
Pt-Ni(2)	93	7
Pt-Ni(3)	92	8
Pt-Ni(4)	90	10

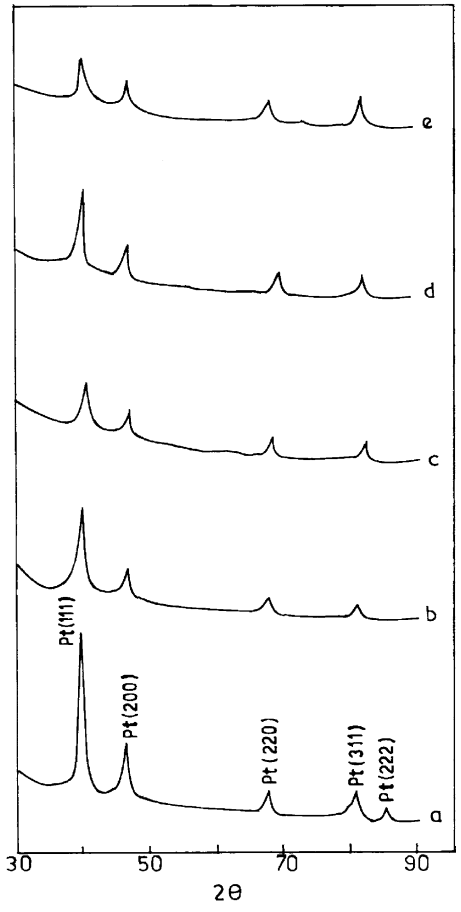

Fig. 1 X-ray diffraction patterns for Pt and Pt-Ni electrodes. *a* Pure Pt, *b* Pt:Ni = 96:4 [Pt-Ni(1)], *c* Pt:Ni = 93:7 [Pt-Ni(2)], *d* Pt:Ni = 92:8 [Pt-Ni(3)], *e* Pt:Ni = 90:10 [Pt-Ni(4)]

Pt peak clearly shows alloy formation between Pt and Ni [29, 30]. Further, the lattice parameters increase up to Pt-Ni(3), and afterwards decrease. The decrease in the lattice constants can be accounted for by the segregation of the alloying elements in the matrix. The substitution of Pt by Ni in the matrix becomes increasingly difficult and hence the decrease in 'd' value may be due to the limited miscibility of Pt with Ni.

Similar observations are reported [31] for Pt-Ni systems which exhibit only a *fcc* structure, with monotonous shift of the diffraction peak positions confirming that Pt and Ni form alloys with solid solution phases, or disordered crystalline structures for this Pt-Ni alloy

Table 2 Parameters derived from XRD patterns

Serial no.	Sample	2 θ	Obs. 'd'	Std. 'd'	hkl	I and I/I_o
01	Pure Pt	39.800	2.263	2.265	111	75/100
	PtNi(1)	40.000	2.252	2.265	111	45/100
	PtNi(2)	40.200	2.241	2.265	111	35/55
	PtNi(3)	40.300	2.236	2.265	111	43/78
	PtNi(4)	40.100	2.247	2.265	111	25/100
02	Pure Pt	46.000	1.971	1.962	200	26/46
	PtNi(1)	46.300	1.959	1.962	200	36/48
	PtNi(2)	46.500	1.951	1.962	200	26/53
	PtNi(3)	46.600	1.947	1.962	200	24/53
	PtNi(4)	46.400	1.955	1.962	200	28/45
03	Pure Pt	67.200	1.392	1.387	220	19/25
	PtNi(1)	68.000	1.387	1.387	220	18/32
	PtNi(2)	69.600	1.357	1.387	220	16/32
	PtNi(3)	70.200	1.334	1.387	220	14/26
	PtNi(4)	68.100	1.376	1.387	220	17/27
04	Pure Pt	80.869	1.188	1.182	311	19/25
	PtNi(1)	80.900	1.187	1.182	311	13/21
	PtNi(2)	81.100	1.185	1.182	311	17/35
	PtNi(3)	81.800	1.176	1.182	311	16/36
	PtNi(4)	81.217	1.183	1.182	311	33/42

formed by sputtering. Thus, XRD analysis shows alloy formation for all the Pt-Ni films, since only Pt *fcc* structure as identified by the diffraction peak shifts from that of pure Pt.

The electrodeposited films are found to be smooth as assessed by scanning electron microscopy carried out after each deposition and the representative micrographs are presented in Fig. 2, Fig. 3, and Fig. 4. In comparison to nanoparticulate films [16], the bulk alloy films are generally smoother.

Figure 5 shows the cyclic voltammetric (first cycle) responses of electrodeposited films of Pt and Pt-Ni in 0.5 M H_2SO_4 solution at $v = 50$ mVs^{-1} in a potential window of −0.65 to 0.70 V versus MSE. It can be seen from the voltammograms (Fig. 1a–e) that the charge densities associated with the reversible hydrogen adsorption-desorption region decrease to a considerable extent upon the inclusion of Ni in the Pt matrix due to

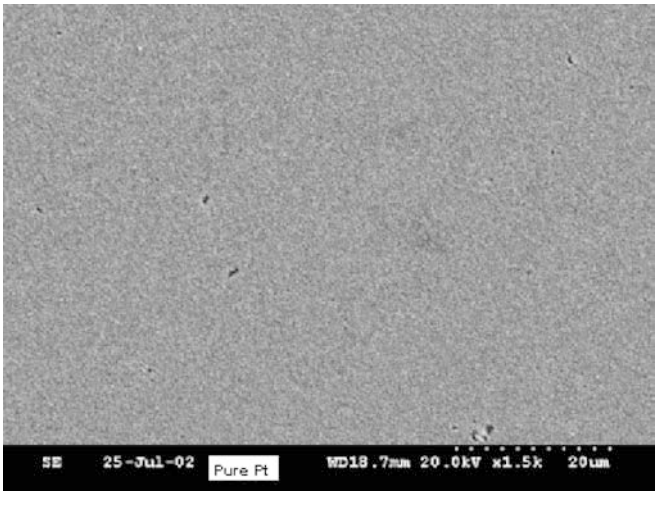

Fig. 2 Scanning electron microscopy (SEM) micrograph of electrodeposited Pt (magnification×1.5 k)

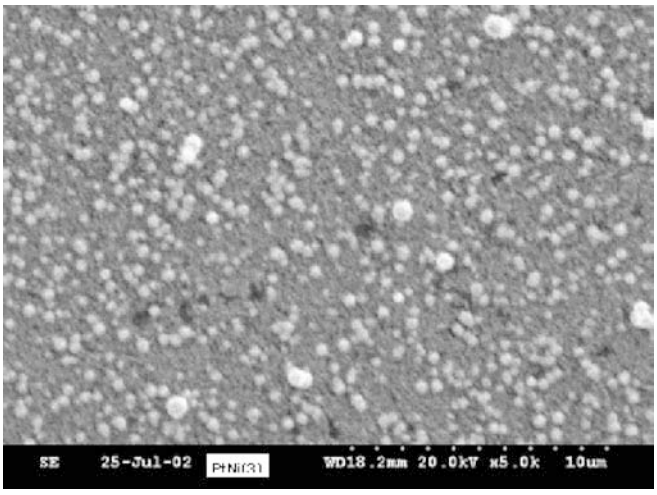

Fig. 3 SEM micrograph of electrodeposited Pt-Ni (Pt-Ni3) (magnification×5.0 k)

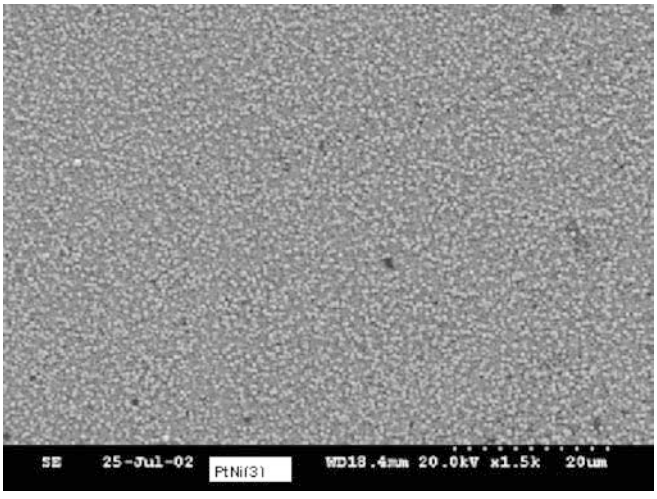

Fig. 4 SEM micrograph of electrodeposited Pt-Ni (Pt-Ni3) (magnification×1.5 k)

the site blocking effect. Inclusion of any foreign metal in the Pt matrix will bring down the charge densities in the H_{upd} region [32], similar to the metal *upd* behaviour. This feature forms the basis for voltammetrically confirming the presence of the metal that alloys with Pt.

Methanol oxidation at electrodeposited Pt-Ni catalysts on Au

Figure 6 shows the polarisation curves of methanol oxidation on electrodeposited Pt and Pt-Ni alloys in 0.5 M H_2SO_4 + 0.5 M CH_3OH in a potential range of −0.25 to 0.30 V versus MSE at a scan rate of 5 mVs^{-1}. It is generally observed that the current values obtained at Pt-Ni alloy surfaces are higher than those of pure Pt, the maximum increase being at the Pt-Ni(3) alloy (∼15 times). Interestingly, matching this observation, the on-

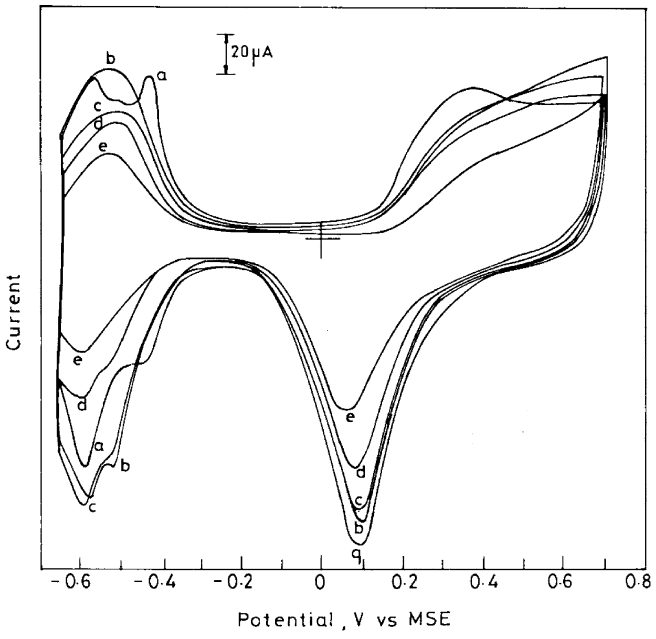

Fig. 5 Cyclic voltammograms of Pt and Pt-Ni electrodeposits in 0.5 M H_2SO_4 at 50 mV s^{-1} sweep rate. *a* Pure Pt, *b* Pt-Ni(1), *c* Pt-Ni(2), *d* Pt-Ni(3), *e* Pt-Ni(4), *MSE* Mercury-mercurous sulphate electrode

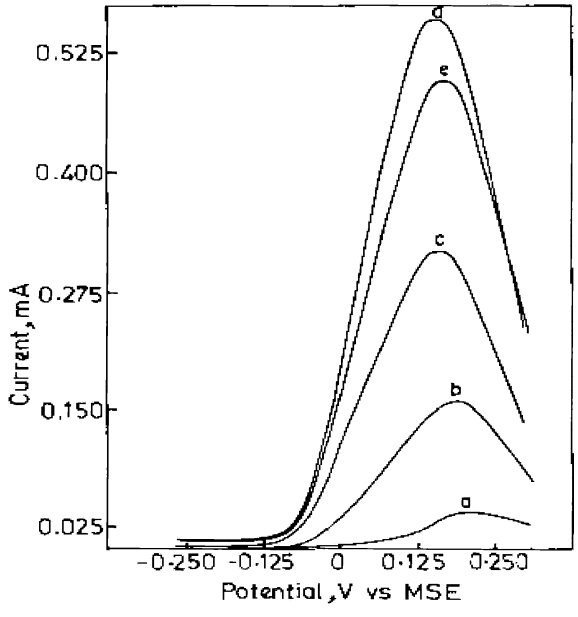

Fig. 6 Polarisation plots for Pt and Pt-Ni electrodeposits on Au for methanol oxidation in 0.5 M CH_3OH + 0.5 M H_2SO_4 with a scan rate of 5 mV s^{-1} at room temperature. *a* Pure Pt, *b* Pt-Ni(1), *c* Pt-Ni(2), *d* Pt-Ni(3), *e* Pt-Ni(4)

set potential for methanol oxidation shifts to less anodic potentials with an increase in the Ni content (Table 3) with a maximum shift (by 160 mV) with reference to the onset potential at pure Pt. Surprisingly, this shift in onset potential is far in excess of the value reported (∼90 mV) for a nanoparticle film of Pt/Ru/Ni (5:4:1) reported by Park et al [20]. In our opinion, this phenomenon may be a

Table 3 Onset potentials for methanol oxidation using Pt and Pt-Ni electrodeposited alloys in 0.5 M methanol + 0.5 M H_2SO_4

PtNi alloy	Onset potential vs MSE (mV)
Pt	+108
Pt-Ni(1)	−31
Pt-Ni(2)	−60
Pt-Ni(3)	−63
Pt-Ni(4)	−60

general feature of Pt-M (M = transition metals/metal oxides) in promoting the electrochemical conversion of CO, thus removing the surface poison, i.e. CO_{ads}. As can be seen from Fig. 4, the current value increases with increasing Ni content. However, the current starts decreasing beyond a critical alloy composition, i.e. Pt-Ni(3). The catalytic activity of the Pt-Ni binary alloy decreases remarkably when the Ni content exceeds 8%. As the Ni composition increases, the number of active Pt sites (Pt*) available for the dissociative chemisorption of the methanol molecule is reduced which causes a reduction in the oxidation current.

Polarisation curves were analysed using the Tafel relationship and the slope values calculated from the linear region are given in Table 4. The observed Tafel slope values, viz., 74 (Pt-Ni-1), 69 (Pt-Ni-2), 90 (Pt-Ni-3) and 78 (Pt-Ni-4) mV decade $(dec)^{-1}$ are lower than the value known for pure Pt surface, i.e. 126 $mVdec^{-1}$(potential-dependent coverage by CO). A value of $\sim$120 $mVdec^{-1}$ is associated with a mechanism in which the oxidative removal of CO_{ads}, in the case of Pt electrodes, is typically an electrochemical rate-determining step (i.e. <130 $mVdec^{-1}$) [33]. The lower slope values show a potential-independent nature of CO coverage, conforming to the earlier observation that the adsorbed CO is susceptible to consumption by nucleophilic attack (the nucleophiles being OH radicals or any species partially arising out of oxidised Ni that may form in the alloy during the methanol oxidation).

Figure 7 shows the current versus time plots with the current normalised to the initial current (i_{meas}/i_o) for the electrodeposited Pt and Pt-Ni alloys in 0.5 M H_2SO_4 + 0.5 M CH_3OH, obtained at a constant potential of 0.18 V versus MSE. For each catalyst composition, the decay of methanol oxidation current is different. For pure Pt deposit, the initial current decays to 20% within 10 min, whereas for the Pt-Ni alloys it took 40 min to decay to 20%. For the Pt-Ni(3) alloy composition, the current crossed 40% only after 50 min.

Table 4 Tafel slopes of methanol oxidation using electrodeposited Pt and PtNi alloys in 0.5 M methanol + 0.5 M H_2SO_4

PtNi alloy	Tafel Slope mV dec^{-1}
Pt	126
Pt-Ni(1)	74
Pt-Ni(2)	69
Pt-Ni(3)	90
Pt-Ni(4)	78

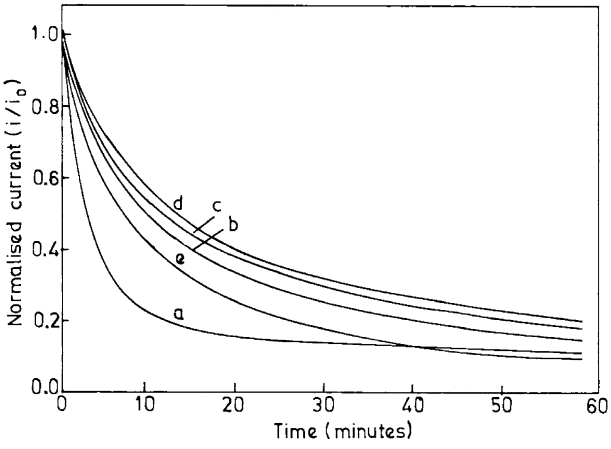

Fig. 7 Current time plot of Pt and Pt-Ni electrodeposits on Au in 0.5 M CH_3OH + 0.5 M H_2SO_4 at a constant potential of 0.18 V vs MSE at 25 °C. *a* Pure Pt, *b* Pt-Ni(1), *c*Pt-Ni(2), *d* Pt-Ni(3), *e* Pt-Ni(4)

The absolute current measured after 1 h for Pt-Ni(3) alloy was 3 orders of magnitude higher than that obtained with pure Pt.

Figure 8 shows the cyclic voltammetric behaviour of electrodeposited Pt and Pt-Ni alloy in 0.5 M H_2SO_4 and

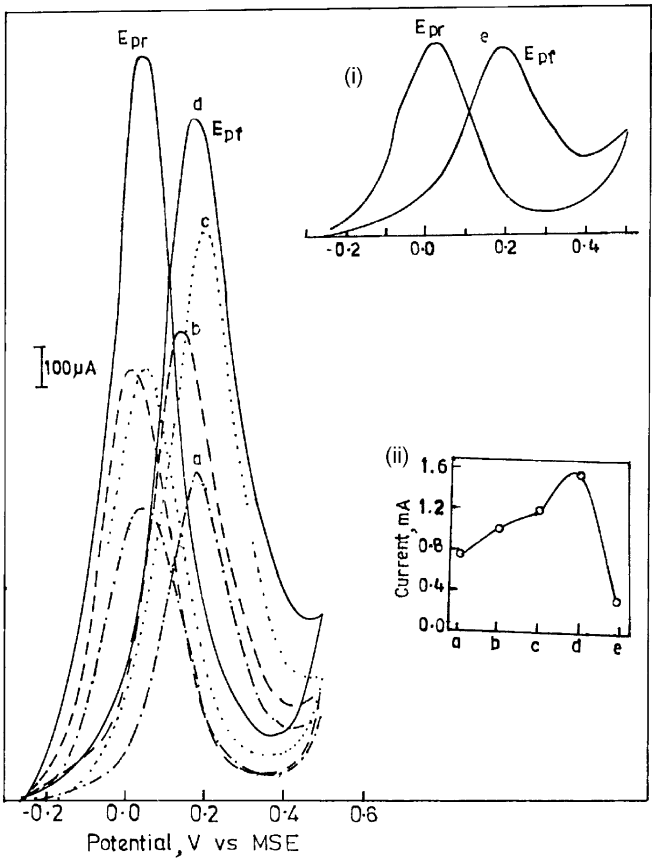

Fig. 8 Cyclic voltammograms of Pt and Pt-Ni electrodeposits in 0.5 M CH_3OH + 0.5 M H_2SO_4 (Sweep rate 50 mV s^{-1}). *Dot-dash line a* Pure Pt, *dash line b* Pt-Ni(1), *dot line c* Pt-Ni(2), *solid line d* Pt-Ni(3). *Inset (i) e* Pt-Ni(4), *inset (ii)* methanol oxidation peak current vs Pt-Ni composition

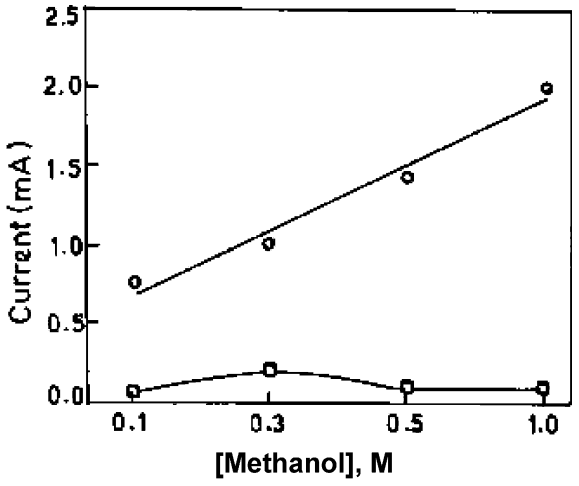

Fig. 9 Anodic peak current vs [methanol]. *Circles* Pt-Ni(3), *squares* polycrystalline Pt

0.5 M CH_3OH at a scan rate of 50 mVs^{-1}. When compared to pure Pt and other Pt-Ni alloys, Pt-Ni(3) alloy yields maximum oxidation current. The anodic peak current increases linearly with Ni content in the alloy matrix and the activity decreases after a critical composition of Pt-Ni(3) as observed in the polarisation studies. A steady increase in the methanol oxidation current and the slope of the polarisation curve Fig. 9 with increasing Ni content show that the effect of surface area on the polarisation characteristics is negligible. This trend matches with the results obtained in the above steady-state polarisation measurements.

The presence of significant peak current in the reverse scan (Ep_r) indicates that active Pt (or Pt oxide) sites exist by the side of Ni or Pt-Ni bimetallic sites, thus suggesting a surface structure similar to an "ensemble" effect [34]. As may be observed in the voltammograms, the potential separation between the peak in the forward- and that in the reverse-scans is reduced from ~200 mV (pure Pt) to ~130 mV. This reduction in peak separation suggests that the initial oxidation of methanol and the consumption of CO_{ads} by OH_{ads} species take place in a narrow potential range, while also reducing the onset potential of methanol oxidation (Fig. 6). The OH_{ads} chemistry (on Pt or Pt-Ni sites) is known to play a key role in promoting methanol oxidation. The interplay between the contributions from (a) electron transfer from Ni to Pt and thus the OH_{ads} reactivity (towards the consumption of CO), and/or (b) the "ensemble" effect, is not currently understood, and has intrigued many researchers in this field. Certainly, this aspect needs more detailed experiments wherein a perfect control over the surface sub-structure (e.g. surface segregation) can be exercised. The recent work of Paulus et al. [35] in the context of oxygen reduction reaction clearly emphasises this point. In our opinion, any ideal electrocatalyst candidate should be in a position to bring about the merger of these two peaks (Ep_f and Ep_r).

It is noteworthy that with Pt-Ni(3), the peak current increases linearly with [MeOH], whereas such a relationship is not observed with polycrystalline Pt. Unfortunately, there are no reports in the literature, to our knowledge, to compare these results. The linear relationship indicates the reduced influence of any adsorbed surface poison on Pt-Ni(3). As methanol oxidation reaction (MOR) is a multistep reaction with possible poisoning of the electrode surface during its oxidation, the peak current is not expected to scale linearly with [MeOH], unless the reaction rate depends linearly on methanol concentration. This observation may have important ramifications for the use of Pt-transition metal alloy catalysts for methanol oxidation. It is also our intent to compile such data to arrive at plots of oxidation current versus [MeOH] on various well-defined catalyst surfaces, in future.

The effects of the alloying element in the Pt based binary alloy on the electro-oxidation reaction of methanol have been satisfactorily explained on the basis of (a) the bifunctional mechanism, (b) the electronic interaction between the alloying element and Pt and (c) the increase in electrochemical active area due to the "leaching out" effect of the alloying element [36, 37]. In this present study, the catalytic role of Ni can be explained by the oxidised Ni species and by the change in the electronic structure of Pt due to the presence of Ni. The role of Ni as a catalytically enhancing agent in the oxidation process is due to the electron transfer from Ni to Pt in the Pt-Ni matrix. The mixed valence of Ni (+2 and +3 states) and its contribution to proton conductivity are akin to the behaviour of hydrous ruthenium oxide (differing in their Fermi levels). While the electronic effects of Ni in the Pt matrix (as Pt-Ni nanoparticles of ~3–4 nm) became evident in the X-ray photo-spectroscopy studies of Park et al. [20], Ni oxide/hydroxide layers within the Pt matrix which are relatively stable in the acidic medium, exhibit protonic/electronic conductivity and such an oxide/hydroxide layer in the Pt-Ni alloy matrix displays high catalytic behaviour with respect to methanol.

The observation that there is a substantial increase in the current of MeOH oxidation suggests consumption of CO in the following steps:

$$\mathrm{CO\text{-}Ni} + \mathrm{OH-Ni} \rightarrow 2\mathrm{Ni} + \mathrm{CO_2} + \mathrm{H^+} + \mathrm{e^-} \quad (1)$$

$$\mathrm{CO\text{-}Pt^*} + \mathrm{OH-Ni} \xrightarrow{\mathrm{rds}} \mathrm{Pt^*} + \mathrm{Ni} + \mathrm{CO_2} + \mathrm{H^+} + \mathrm{e^-} \quad (2)$$

$$\mathrm{CO\text{-}Pt} \rightarrow \mathrm{CO\text{-}Pt^*} \quad (3)$$

$$\mathrm{Ni} + \mathrm{H_2O} \rightarrow \mathrm{Ni-OH} + \mathrm{H^+} + \mathrm{e^-} \quad (4)$$

where, Pt* = active Pt site on the catalytic surface.

While it is reasonable to think that all transition metals should be able to behave like Ru in their hydrous oxide forms (as required for the oxygenation of CO), a comparison among such alloying elements (with Pt)

would be a worthwhile exercise. Since bulk conversion of Ni to its $+2/+3$ state requires its oxidation in alkaline medium [24], a surface redox film of $Ni(OH)_2$/NiOOH is reported to be sufficient to favour methanol oxidation in acid medium. As control experiments, a comparison of the electrochemical cycling behaviour of Pt-Ni deposits in alkaline (from 0.13 V to 0.6 V vs SCE) and acid media (from 0.13 V to 0.8 V vs SCE) revealed the following facts: (a) only in alkaline medium (0.1 M NaOH), bulk Ni dissolution currents were observed, as identified by the "signature response" of $Ni(OH)_2$/NiOOH transition (as in [24]), whereas in (b) acid medium, no features of oxidative dissolution were found that exhibit this transition.

The above mechanism (Eq. 1, Eq. 2, Eq. 3, Eq. 4) also indicates that electron transfer from Ni to Pt is possible, as supported by earlier work [20]. It is known from literature that pure Ni dissolution takes place at potentials of $E < 0.6$ V versus MSE in acid solution [38]. No apparent dissolution of Ni in the Pt-Ni in any of its compositions was observed voltammetrically in the potential range of methanol oxidation. This is also reflected in the absence of reversible peak pattern typical of Ni-oxide/hydroxide conversion [24] in cyclic voltammetry. However, Ni dissolution in acid medium in the potential region of methanol oxidation is likely to yield a surface redox consisting of $Ni(OH)_2$/NiOOH. Whatever dissolution is possible will be limited since the source of Ni is from the Pt lattice. Hence, there is sufficient reason to believe that the Pt lattice in acidic media can stabilise Ni in the Pt-Ni deposit. The ultimate index of performance of these types of alloys is their long-term stability to match or exceed the performance of Ru and future studies should address issues such as the additional roles that can be played by metals such as Ni, Co, Mo, W, etc. as already done by Ir, Os, Ru [39, 40]. Certainly, there remains much more to be explored in this area. In the absence of predictive theories for the selection of electrocatalysts, there is no alternative to experimentation with various possible alloying elements.

Conclusions

Using electrodeposition, smooth deposits of Pt-Ni alloys of various compositions were obtained on Au substrate. The elemental analysis (XRF) and powder X-ray diffraction studies showed the formation of Pt-Ni alloys (solid solutions). These electrodeposited alloy films were evaluated for oxidation of methanol in 0.5 M H_2SO_4 solutions, using (a) steady-state polarisation, (b) cyclic voltammetry, and (c) chronoamperometry.

From the steady-state polarisation studies in 0.5 M methanol in 0.5 M H_2SO_4 solutions, it is clear that with increase in the Ni content of the Pt-Ni alloy:

1. The onset of electro-oxidation shifts to less anodic potential values (by ~160 mV).
2. Current enhancements up to ~15 times on compared with the currents observed for the pure Pt electrodeposit and the following observations confirm the electrocatalytic activity of the deposited layers.
3. The normalised current measured after 1 h in chronoamperometry experiments is 3 orders of magnitude higher for the Pt-Ni(3).
4. A linear relationship between the oxidation current and [MeOH] was observed, thus indicating reduced influence of CO_{ads} surface poison. A critical composition, Pt (92%)/Ni (8%) [Pt-Ni(3) alloy] was found to exhibit maximum electrocatalytic activity (based on the shift in onset potential), beyond which the activity drops whereas pure Ni did not catalyse the reaction, as observed by us and Park et al. [20].

Since the current work and work carried out elsewhere confirms that the electrochemical promotion of oxidation of small molecules (specifically, methanol) is likely a general behaviour of the transition metal alloys of Pt, it now remains to be seen if the catalytic activity can be increased by using supported (e.g. on carbon) nanoparticle films. A comparison of the behaviour of these nanoparticle films versus atomically smooth [41] alloy deposits will be able to reveal the true power of nanoparticles as electrocatalysts.

Acknowledgements AMR thanks CSIR, India for a Senior Research Fellowship and K.L.N.P. thanks Department of Science & Technology, India for financial support (SP/S1/H-20/99). The authors are thankful to the referees for their constructive suggestions.

References

1. Wantanabe M, Mooto S (1975) J Electroanal Chem 60:267
2. Lipkowski J, Ross PN (1998) Electrocatalysis. Wiley-VCH, NewYork
3. Parsons R, VanderNoot T (1998) J Electroanal Chem 257:257
4. Wieckowski A (1999) Interfacial electrochemistry—theory, experiment and applications. Dekker, NewYork
5. Crown A, Moraes IR, Wieckowski A (2001) J Electroanal Chem 500:33
6. Gonzalez MJ, Peters CH, Wrighton MS (2001) J Phys Chem B 105:5470
7. Luo J, Lou Y, Maye MM, Zhong CJ, Hepel M (2001) Electrochem Commun 3:172
8. Okada T, Suzuki Y, Hirose T, Toda T, Ozawa T (2001) Chem Commun 2492
9. Waszczuk P, Solla-Gollan J, Kim HS, Tong YY, Montiel V, Aldaz A Wieckowski A (2001) J Electroanal Chem 203:1
10. Gasteiger HA, Markovic N, Ross PN, Cairns EJ (1993) J Phys Chem 47:12020
11. Goodenough JB, Hamnett A, Kennedy BJ, Manoharan R, Weeks SA (1998) J Electroanal Chem 240:133
12. Rolison DR, Hagans PL, Swider KE, Long JW (1999) Langmuir 15:774
13. Takasu Y, Itaya H, Iwazaka T, Miyoshi R, Ohnuma T, Sugimoto W, Murakami Y (2001) Chem Comm 1:341
14. Gasteiger HA, Markovic N, Ross Jr PN, Cairns EJ (1994) J Phys Chem 48:617
15. Abraham FF, Tsai NH, Pound GM (1979) Surf Sci 83:406
16. Rolison DR, Hagans PL, Swider KE, Long JW (1999) Langmuir 15:774
17. Long JW, Stroud RM, Swider-Lyons KE, Rolison DR (2000) J Phys Chem B 104:9772

18. Gurau B, Viswanathan R, Liu RX, Lafrenz TJ, Ley KL, Smotkin ES, Reddington E, Sapienza A, Chau BC, Mallouk TE, Sarangapani S (1998) J Phys Chem B 102:9997
19. McNicol BD, Short RT (1977) J Electroanal Chem 81:249
20. Park KW, Choi JH, Kwon BK, Lee SA, Sung YE, Ha HY, Hong SA, Kim H, Wieckowski A (2002) J Phys Chem B 106:1869
21. Manoharan R, Goodenough JB (1992) J Mater Chem 2:875
22. Drillet JF, Friedemann AEeJ, Kotz R, Schnyder B, Schmidt VM (2002) Electrochim Acta 47:1983
23. Kowal A, Port SN, Nichols RJ (1997) Catal Today 38:483
24. El-Shafei AA (1999) J Electroanal Chem 471:89
25. Beden B, Leger JM, Lamy C (1992) Electrochemical oxidation of oxygenated aliphatic organic compounds at noble metal electrodes. In: BockrisJ.O'M, Conway BE, White RE (eds) Modern aspects of electrochemistry, vol. 22. Plenum, New York, pp 97–247
26. Stamenkovic V, Schmidt TJ, Ross PN, Markovic NM (2002) J Phys Chem B 106:11970
27. Schonenberger C, Vanderzande BMI, Fokkink LG, Henny M, Schmid C, Kruger M, Bachtold A, Huber R, Birk H, Sranfer U (1997) J Phys Chem B 101:5497
28. Sobkowski J, Franaszczuk K, Piasecki A (1985) J Electroanal Chem 196:145
29. Liu R, Ley KL, Pu C, Fan O, Leyarovska N, Segre C, Smotkin ES (1996) Bifunctional Pt-Ru-Os ternary alloys—improved Pt-based anode for direct methanol fuel cells. In: Wieckowski A, Itaya K (eds) Electrode Processes VI. The Electrochemical Society; Pennington, N.J., pp. 341
30. Deivaraj TC, Chen W, Lee JY (2003) J Mater Chem 13:2555
31. Toda T, Igarshi H, Uchida H, Wantanabe M (1999) J Electrochem Soc 146:3750
32. Bakos I, Szabo S (2001) Electrochim Acta 46:2507
33. Schmidt TJ, Gasteiger HA, Behm RJ (1999) Electrochem Commun 1:1
34. Ross PN (1998) The science of electrocatalysis on bimetallic surfaces. In: Lipkowski J, Ross PN (eds) Electrocatalysis. Wiley-VCH, NewYork, p 72
35. Paulas UA, Wokaun A, Scherer GG, Schmidt TJ, Stamenkovic V, Markovic NM, Ross PN, (2002) J Phys Chem B 106:4181
36. Wasmus S, Kuver A (1999) J Electroanal Chem 461:14
37. Carrette L, Friedrich KA, Stimming U (2000) Chem Phys Chem 1:162
38. Barnett J, Burstein GT, Kucernak AR, Williams KR (1997) Electrochim Acta 42:2381
39. Jusys Z, Schmidt TJ, Dubau L, Lasch K, Jorissen L, Garche J, Behm RJ (2002) J Power Sources 105:297
40. Wang H, Wingender C, Baltruschat H, Copez M, Reetz MT (2001) J Electroanal Chem 509:163
41. Friedrich KA, Geyzers KP, Dickinson AJ, Stimming U (2001) J Electroanal Chem 524–525:261